INFN
Istituto Nazionale
di Fisica Nucleare
SEZIONE DI PISA

Angela Bonaccorso
bonac@df.unipi.it

Pisa: Torre Pendente

Single particle states in the continuum

D. M. Brink, G. Blanchon, N. Vinh Mau

- For bound states $C^2S=\sigma_{exp}/N\sigma_{th}$ from transfer and/or breakup reactions.
- For continuum states spectroscopic strength $S(\varepsilon)$, n-target(core) interaction is complex, energy dependent and single particle states have $\longrightarrow$ $\Gamma = \Gamma_0 + \Gamma^{\downarrow}$
- Final state interaction theory (Fermi, Watson…)
- Examples : low-lying resonances in ^{209}Pb,
  the problem of ^{10}Li , ^{13}Be ground state $\longrightarrow$ ^{11}Li, ^{14}Be

$\longrightarrow$ (cf. Blanchon talk)

Review of spectra which can be reproduced with the transfer to the continuum theory

J.Enders et al.

PHYSICAL REVIEW C **65** 034318

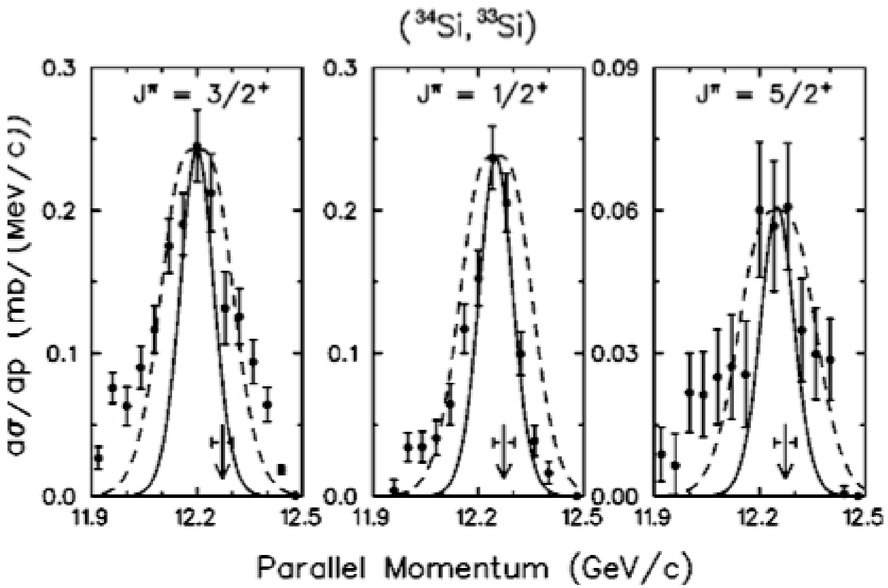

FIG. 3. Parallel-momentum distributions of the reaction residues

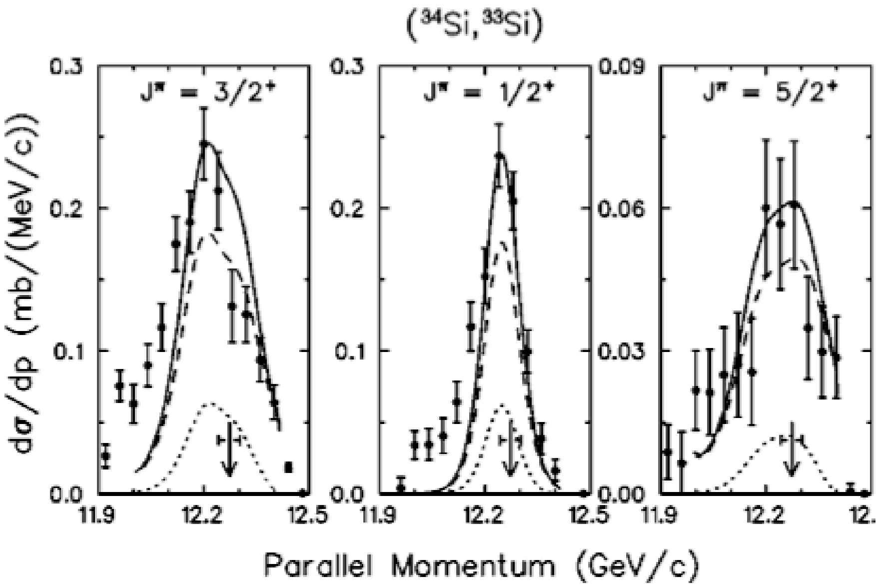

FIG. 4. Measured momentum distribution (full points) co

PHYSICAL REVIEW C VOLUME 51, NUMBER 2 FEBRUARY 1995

High energy single particle states in the continuum

Angela Bonaccorso*

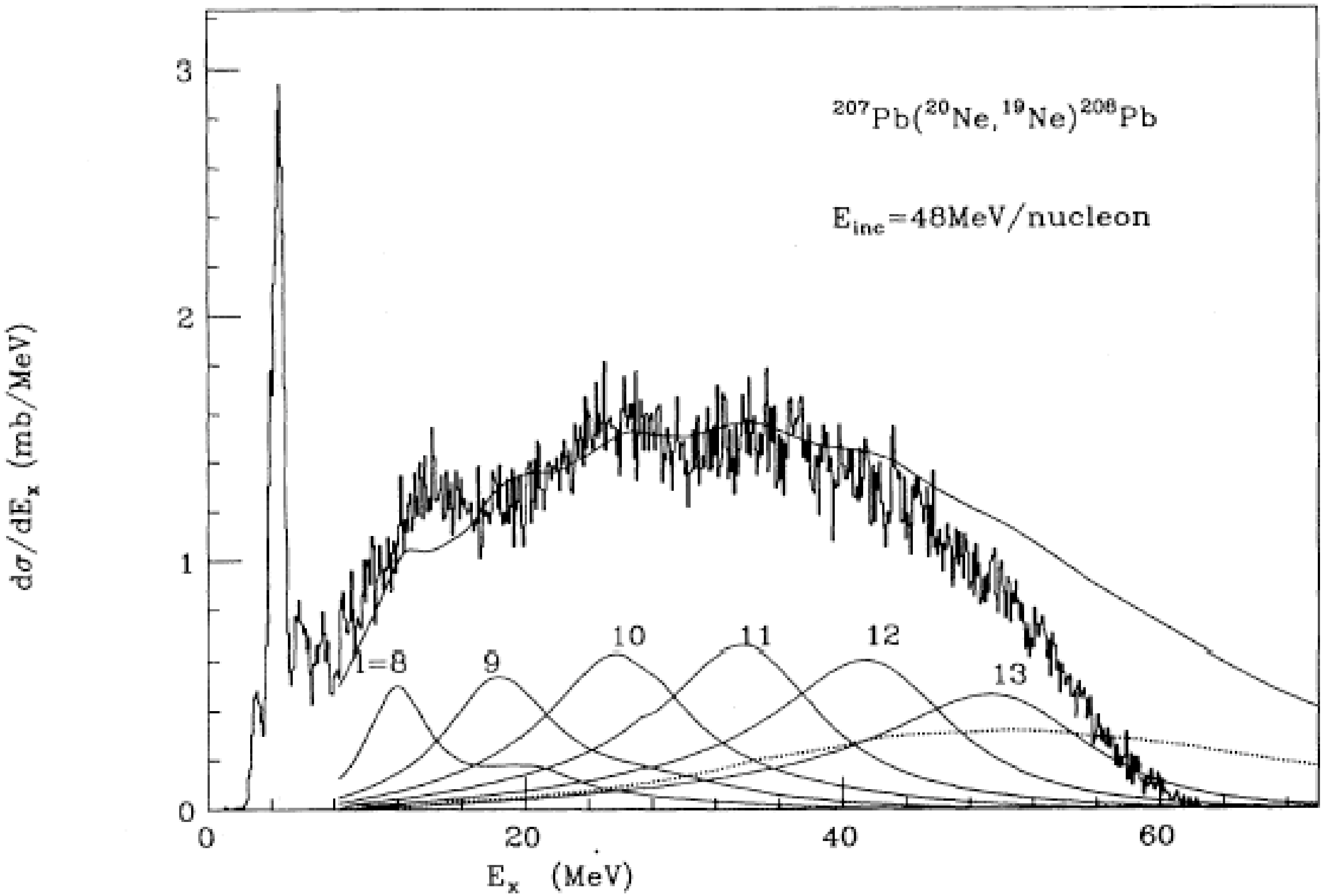

PHYSICAL REVIEW C VOLUME 49, NUMBER 1 JANUARY 1994

Inclusive spectra of stripping reactions induced by heavy ions

A. Bonaccorso
Istituto Nazionale di Fisica Nucleare, Sezione di Pisa, 56100 Pisa, Italy

I. Lhenry and T. Suomijärvi
Institut de Physique Nucléaire, Centre National de la Recherche Scientifique–Institut National de Physique Nucleàire et de Physique des Particules F91406 Orsay, France

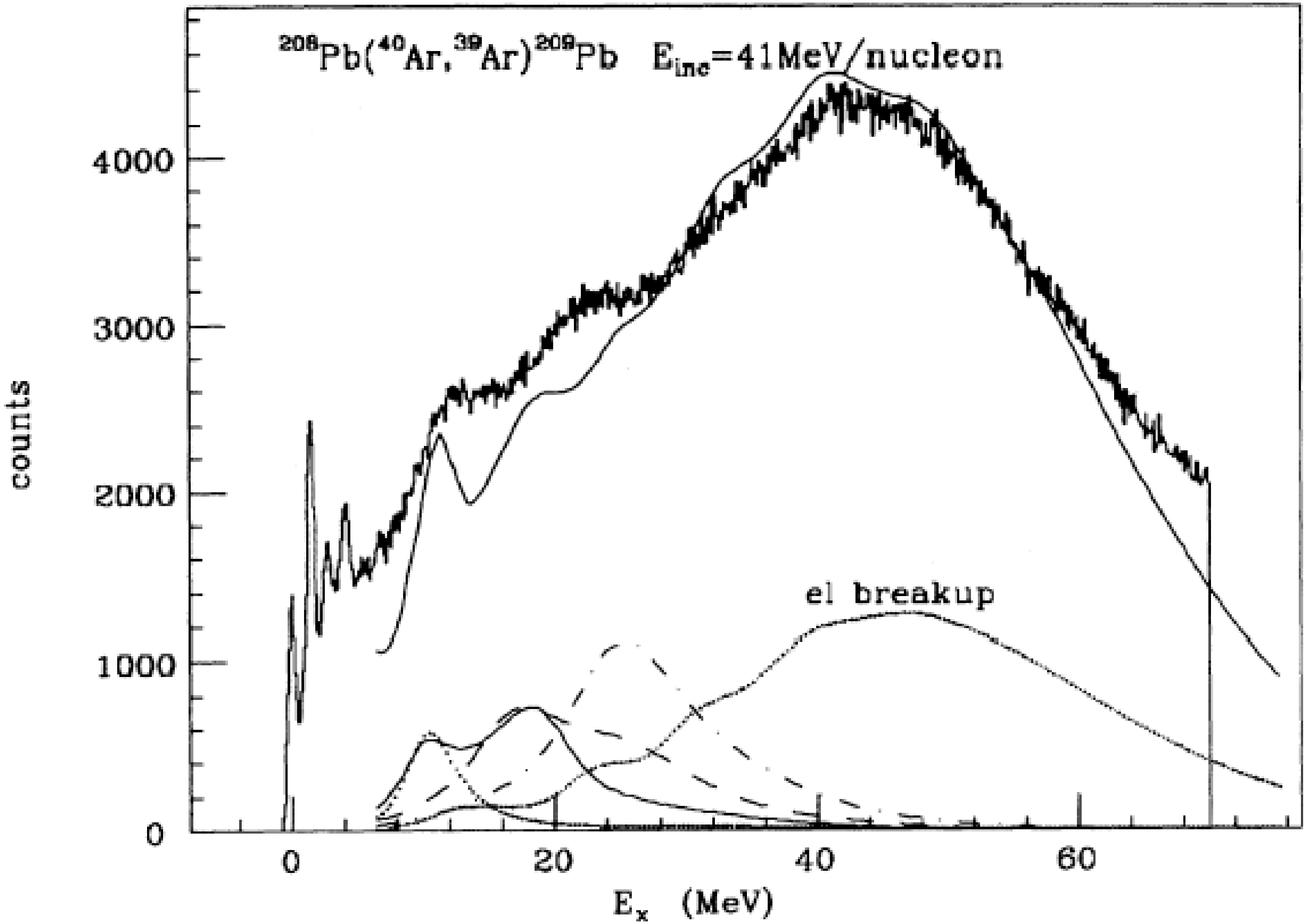

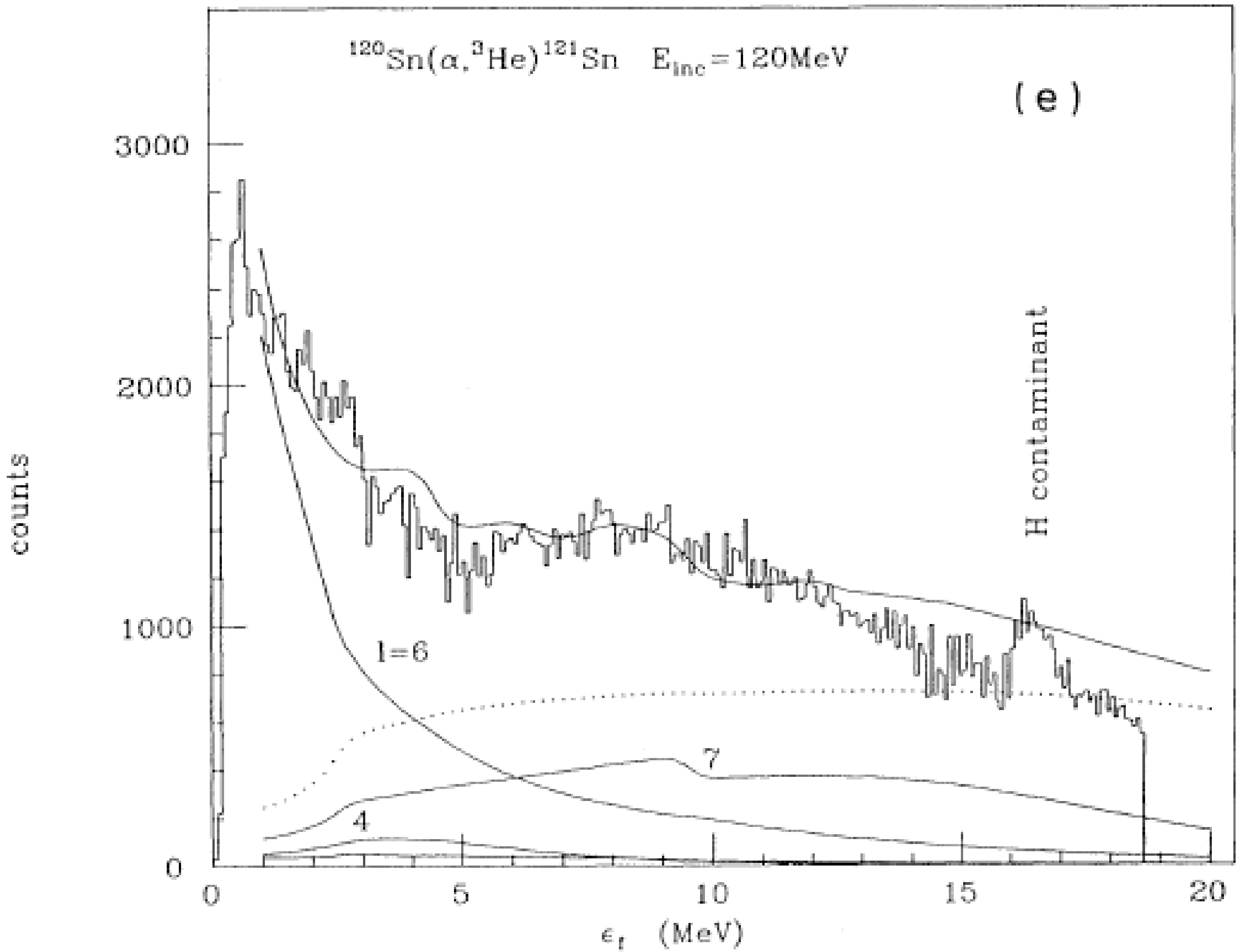

$^{120}Sn(\alpha,{}^{3}He)^{121}Sn$ E_{inc}=120MeV
(e)
H contaminant
counts
3000
2000
1000
0
l=6
7
4
0
5
10
15
20
ϵ_f (MeV)

Where do we stand?…just an example…..

PHYSICAL REVIEW C VOLUME 49, NUMBER 1 JANUARY 1994

Low-lying structure of ^{10}Li in the reaction ^{11}B(^{7}Li,^{8}B)^{10}Li

B. M. Young, W. Benenson, J. H. Kelley, N. A. Orr,* R. Pfaff, B. M. Sherrill, M. Steiner, M. Thoennessen,
J. S. Winfield, J. A. Winger,† S. J. Yennello,† and A. Zeller
National Superconducting Cyclotron Laboratory and Department of Physics and Astronomy, Michigan State University, East Lansing, Michigan 48824

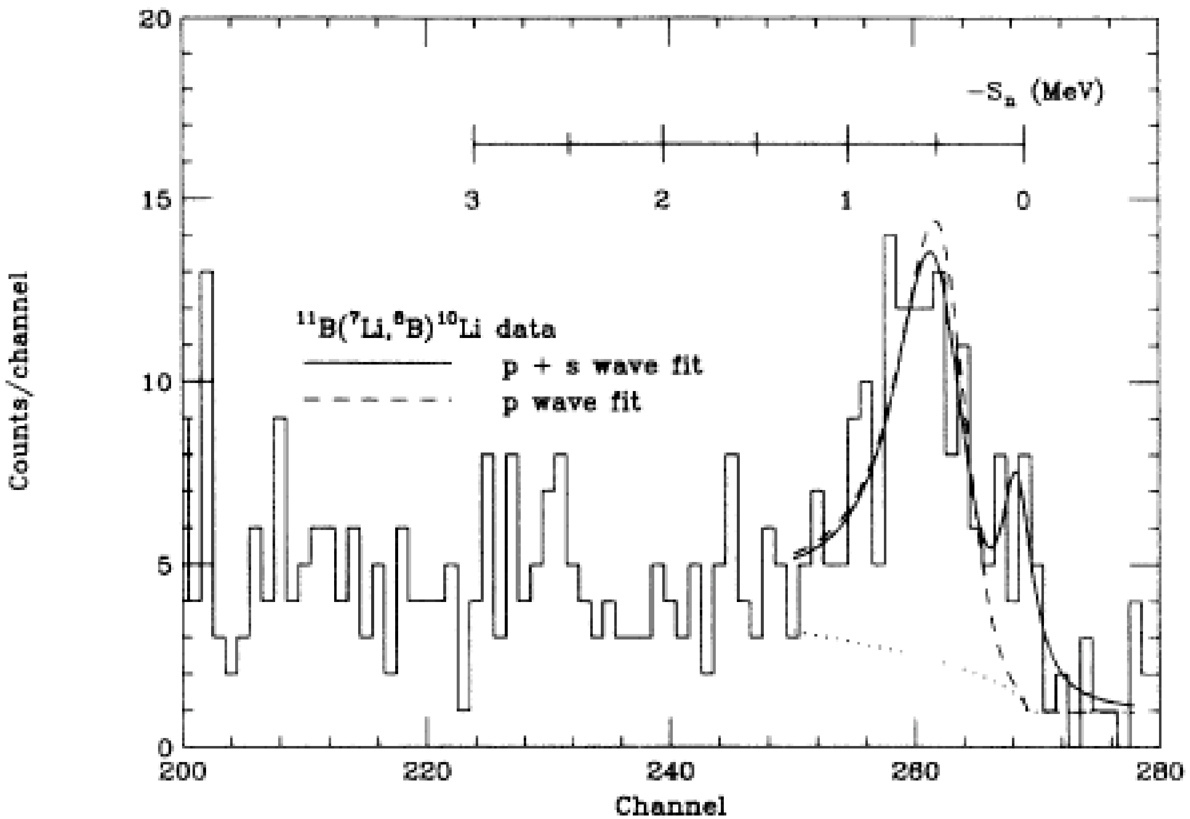

Transfer to the continuum dynamics

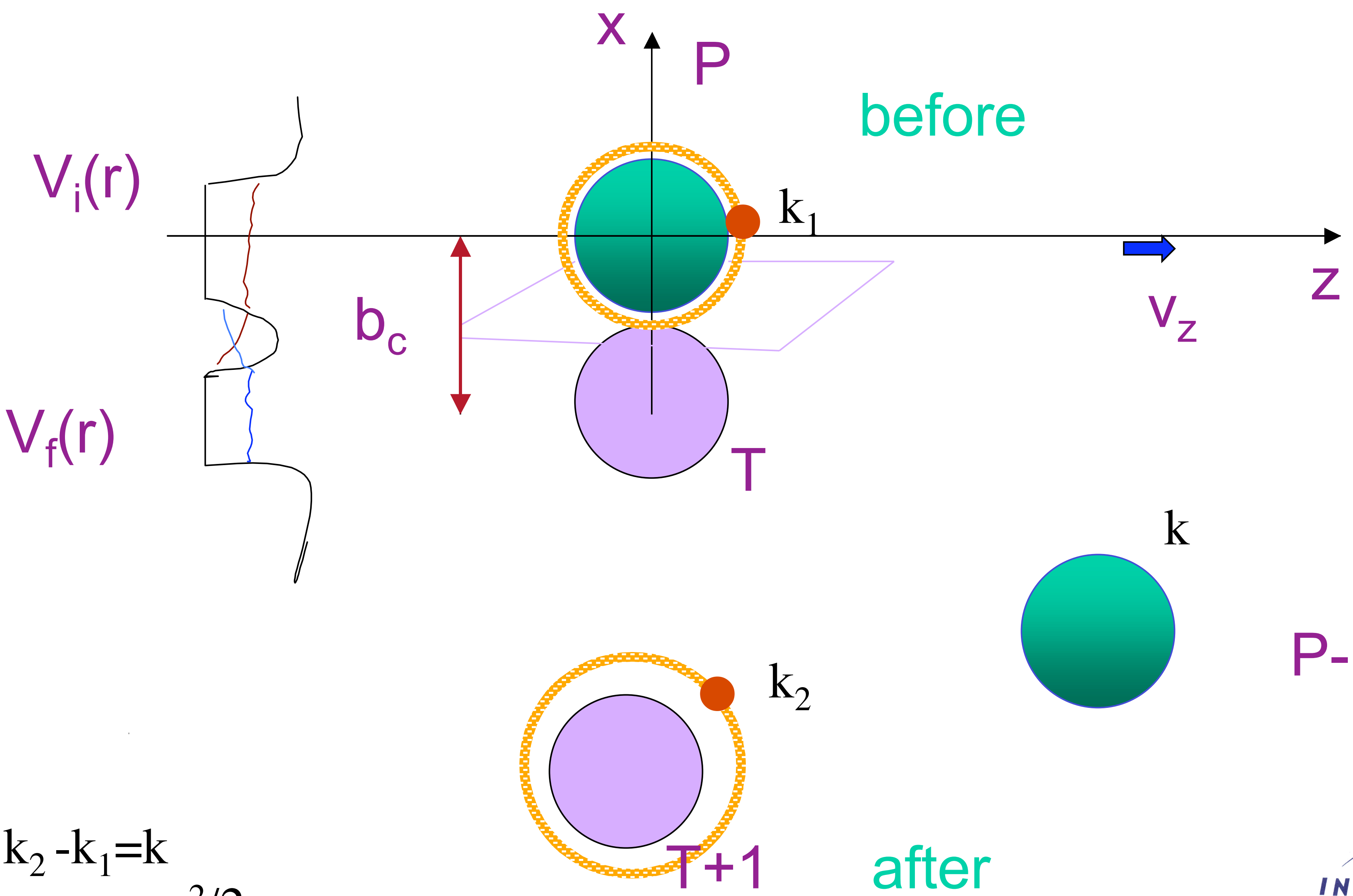

$k_2 - k_1 = k$

$\varepsilon_f - \varepsilon_i = mv^2/2$

DWBA in the CONTINUUM

Semiclassical treatment of core-target relative motion, BUT full QM treatment of n-target interaction

AB and DM Brink, PRC38, 1776 (1988), PRC43, 299 (1991),PRC44, 1559 (1991).

$$\frac{d\sigma}{d\varepsilon_f} = C^2 S \int_0^\infty d\mathbf{b_c} \, \frac{dP(b_c)}{d\varepsilon_f} \, P_{el}(b_c), \qquad \text{where} \qquad P_{el}(b_c) = |S_{cT}|^2$$

$$A_{if} = \frac{1}{i\hbar} \int \, dt < \psi_f(t)|V(r)|\psi_i(t) >$$

$$V(r) = U(r) + iW(r)$$

A study of semi-classical approximations for heavy ion transfer reactions, H. Hasan and D.M. Brink, J Phys G4, 1573 (1978).
Perturbation approach to nucleon transfer in heavy ion reactions, L. Lo Monaco and D.M. Brink, J.Phys. G, 935 (1985).

INFN Istituto Nazionale di Fisica Nucleare SEZIONE DI PISA

The neutron Schrödinger equation

$$i\hbar\frac{\partial\Phi}{\partial t} = (T + V_1(r_1,t) + V_2(r_2,t) + V_C(r_1, R(t))\Phi(t)$$

$$A_{12} =< \Phi_{2\,out}(t_2)|G_2V_2G_1|\Phi_{1\,in}(t_1) >$$

$$A_{11} =< \Phi_{2\,out}(t_2)|G_1V_2G_1|\Phi_{1\,in}(t_1) >$$

$$A_{01} =< \Phi_{2\,out}(t_2)|G_0V_2G_1|\Phi_{1\,in}(t_1) >$$

Istituto Nazionale di Fisica Nucleare

SEZIONE DI PISA

$$\psi_i(r,t) = \phi_i(r) e^{-\frac{i}{\hbar}\varepsilon_i t}$$

$$\psi_f^*(r,t) = \phi_f^*(r) e^{\frac{i}{\hbar}\varepsilon_f t}$$

$$\phi_i(r) = -C_i \gamma_i h_{l_i}^{(+)}(i\gamma_i r) Y_{l_i m_i}(\theta,\phi)$$

$$\phi_f(r) = C_f k_f \frac{i}{2}[h_{l_f}^{(+)}(k_f r) - S_{l_f}^* h_{l_f}^{(-)}(k_f r)] Y_{l_f m_f}(\theta,\phi)$$

$$A_{if}(\mathbf{k_f}, b_c) \approx \int dk_y \sqrt{k_y^2 + \eta^2}\, \bar{\phi}_i(d_1, k_y, k_1) \bar{\phi}_f^*(d_2, k_y, k_2)$$

Istituto Nazionale di Fisica Nucleare
SEZIONE DI PISA

standing the transfer and breakup mechanisms and the best matching ions

$$\frac{dP_t(b_c)}{d\varepsilon_f} = \frac{1}{8\pi^3}\frac{mk_f}{\hbar^2}\frac{1}{2l_i+1}\Sigma_{m_i}|A_{fi}|^2$$

$$\approx \frac{4\pi}{2k_f^2}\Sigma_{j_f}(2j_f+1)(|1-\bar{S}_{j_f}|^2 + 1 - |\bar{S}_{j_f}|^2)(1+F_{l\to j})B_{l_f,l_i}$$

elastic absorption

$$= \sigma_{nN}(\varepsilon_f)\mathcal{F},$$

enhancement factor of of final state interaction theory

$$B_{l_f,l_i} = \frac{1}{4\pi}\left[\frac{k_f}{mv^2}\right]|C_i|^2\frac{e^{-2\eta b_c}}{2\eta b_c}M_{l_f l_i}$$

angular parts of $\psi_{i,f}$

$k_f \equiv (i\eta, k_z)$

$|\tilde{\psi}_i|^2$ Fourier transform of initial w. f.

$$P(l_f,l_i)=\int \frac{dP}{d\varepsilon}(l_f,l_i)d\varepsilon$$

$$\left|\sin\delta_{l_f}\right|^2=\frac{\Gamma}{2}\,\frac{\Gamma/2}{(\varepsilon-\varepsilon_{\rm res})^2+\Gamma^2/4}\simeq\frac{\Gamma}{2}\pi\delta(\varepsilon-\varepsilon_{\rm res})$$

$$\simeq\frac{\Gamma}{2}\pi\int d\varepsilon\,\delta(\varepsilon-\varepsilon_{\rm res})4B(l_{\rm res},l_i)$$

$$=\frac{\pi}{2}\left[\frac{\hbar}{mv}\right]^2\frac{m\Gamma}{\hbar^2 k_{\rm res}}\left|C_i\right|^2(2l_f+1)$$

$$\times P_{l_i}\left[1+2\frac{k_1^2}{\gamma^2}\right]P_{l_f}\left[2\frac{k_2^2}{k_{\rm res}^2}-1\right]\frac{e^{-2\eta R}}{\eta R}\ , \qquad \text{(3.2}$$

where $B(l_{\rm res},l_i)$ is given by Eq. (2.29).

In the case of transfer between bound states [cf. Eq (3.15) of Ref. 4] the equivalent of Eq. (3.2) was

$$P(l_2,l_1)=\frac{\pi}{2}\left[\frac{\hbar}{mv}\right]^2\left|C_1C_2\right|^2(2l_2+1)P_{l_1}\left[1+2\frac{k_1^2}{\gamma_1^2}\right]$$

$$\times P_{l_2}\left[2\frac{k_2^2}{\gamma_2^2}+1\right]\frac{e^{-2\eta R}}{\eta R}\ . \qquad \text{(3.3}$$

Bound to continuum

If both initial and final state have l=0

$$\frac{d\sigma}{dk_f} = (\sin\delta_0)^2 |C_i|^2 \left[\frac{\hbar}{mv}\right] \int_0^{\infty} d\mathbf{b_c} \frac{e^{-2\eta b_c}}{\eta b_c} e^{(-\ln 2 \exp[(R_s - b_c)/a])}.$$

Scattering length

$$a_s = - \lim_{k \to 0} \frac{tan\delta_0}{k}$$

$$|C_2|^2 = \frac{\psi^2_{\mathrm{num}}(R)}{[\gamma_2 h_l^{(+)}(i\gamma_2 R)]^2},$$

$$\frac{m\Gamma}{\hbar^2 k_{\mathrm{res}}} = \frac{u_l^2(R)}{[k_{\mathrm{res}} O_l(k_{\mathrm{res}} R)]^2}.$$

$$k_1 = -\frac{\varepsilon_i - \varepsilon_f + \frac{1}{2}mv^2}{\hbar v}$$

$$k_2 = -\frac{\varepsilon_i - \varepsilon_f - \frac{1}{2}mv^2}{\hbar v}.$$

$$\eta^2 = \gamma_i^2 + k_1^2 = k_2^2 - k_f^2$$

$$\gamma_i^2 = -\frac{2m\varepsilon_i}{\hbar^2}$$

$$k_f^2 = \frac{2m\varepsilon_f}{\hbar^2}$$

$$\mathbf{k_f} \equiv (\mathbf{k}_\perp, k_\mathbf{z}) = (i\eta, k_2)$$

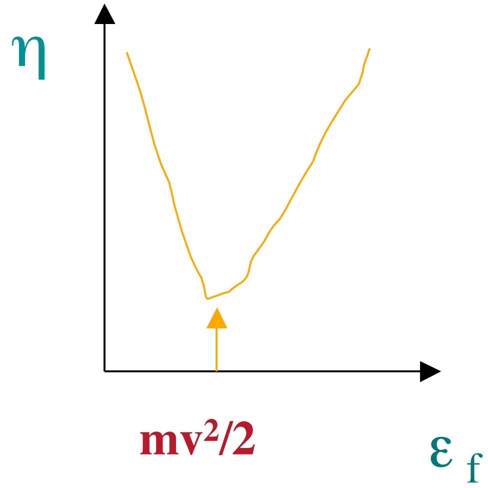

TABLE III. Resonance energies in ^{208}Pb.

l_f	6	7	8	9	10
$\varepsilon_{\mathrm{res}}$ (MeV)	3.2	4.8	5.5	12	19

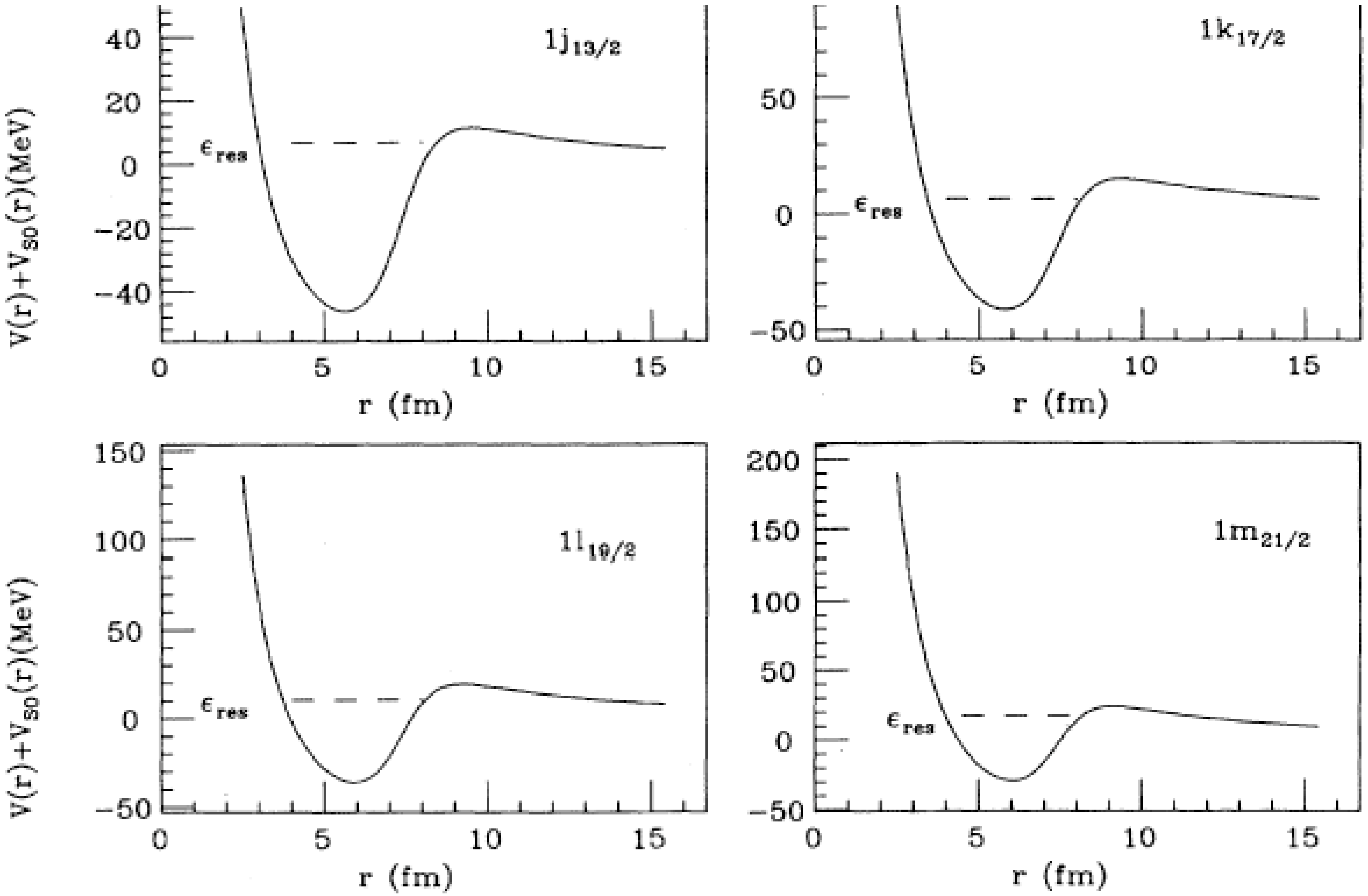

n-^{208}Pb Optical potential from Mahaux and Sartor NP A493 (1989) 157

$$V_R = -45.8 - (0.3\varepsilon_f - 3), \quad \varepsilon_f = 1\text{–}10 \text{ M}$$

$$V_R = -45.8, \quad \varepsilon_f = 10\text{–}20 \text{ MeV},$$

$$V_R = -45.8 + (0.1\varepsilon_f - 1), \quad \varepsilon_f > 20 \text{ Me}$$

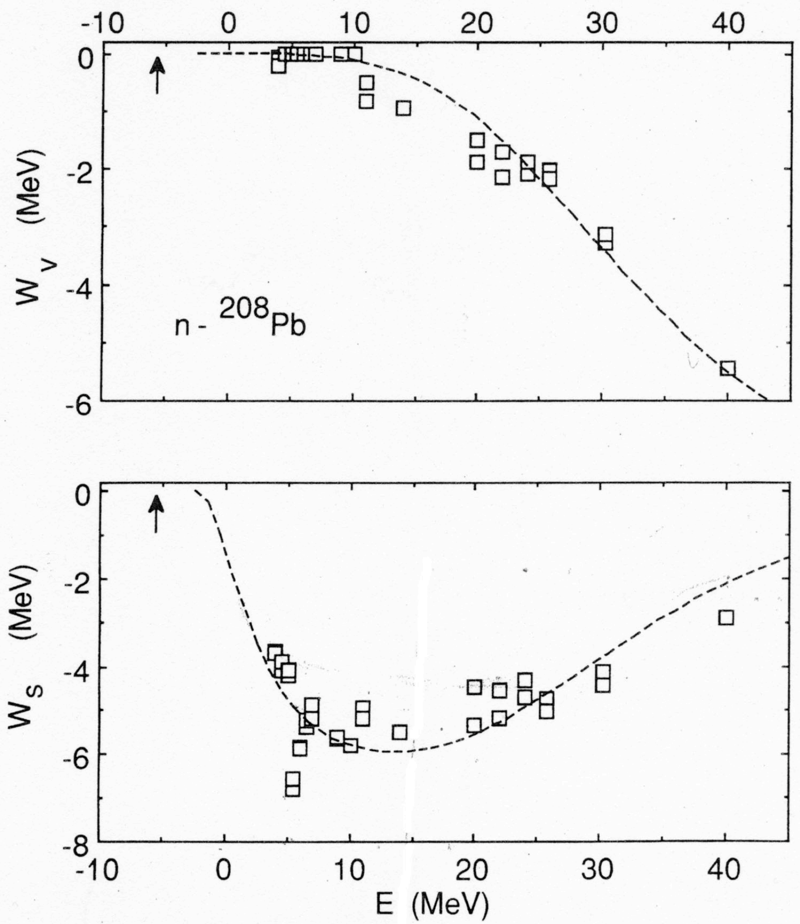

Fig. 7.1. Energy dependence of the strength of the volume and surface absorptions in the case of the *n*-^{208}Pb system. The squares represent "empirical strengths" deduced from the radial moments $[r]_W$ and $[r^3]_W$ associated with the phenomenological optical-model potentials used in Fig. 4.1. The curves represent the parametrization specified by Eqs. (7.14c)–(7.14f). The arrows show the location of the Fermi energy $E_F = -5.65$ MeV.

Potential model for n+^{9}Li continuum

$U(r)=V_{WS}+\alpha\,\delta V$

Woods-Saxon+surface-vibration coupling

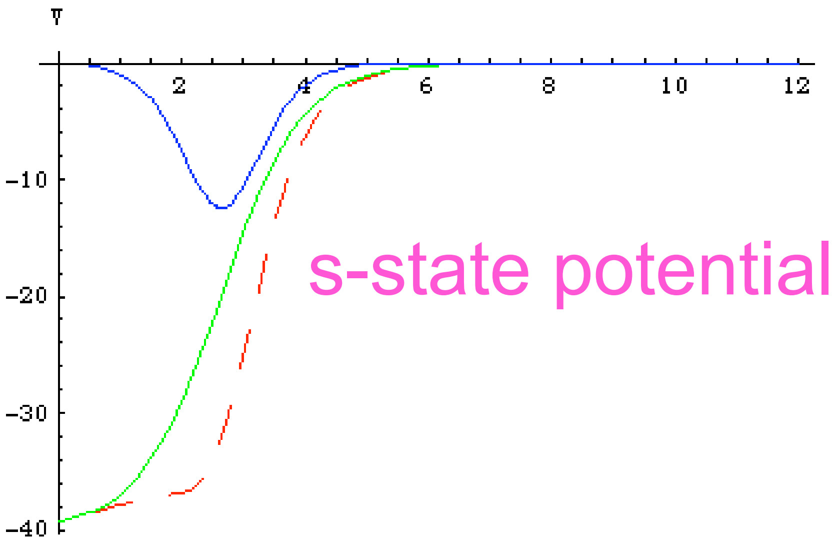

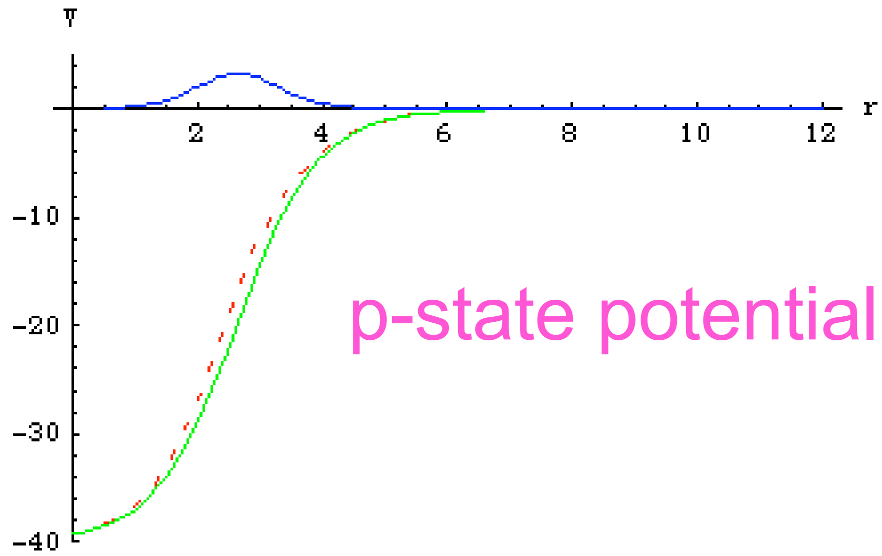

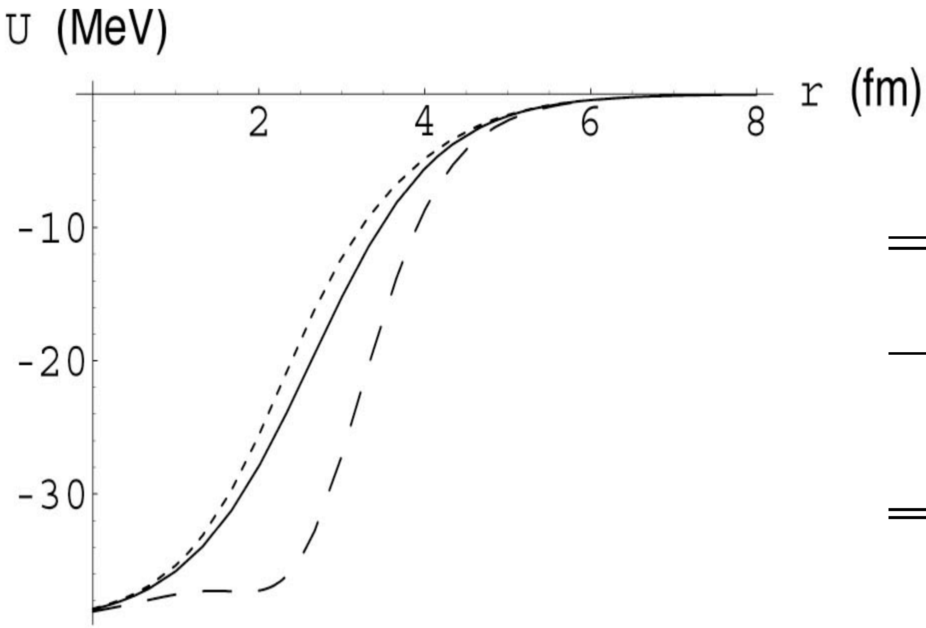

Resonance states in ^{10}Li

	ε_{res} (MeV)	Γ (MeV)	a_s (fm)	α (MeV)
$2s_{1/2}$			323	-12.5
			-17.20	-10.0
$1p_{1/2}$	0.595	0.48		3.3

INFN Istituto Nazionale di Fisica Nucleare SEZIONE DI PISA

Does the volume part of the immaginary potential represent the effects of short range effects?

If there is no absorption and the potential is just real what effects are we taking into account, for example if there is a strong surface correction from vibrational couplings?

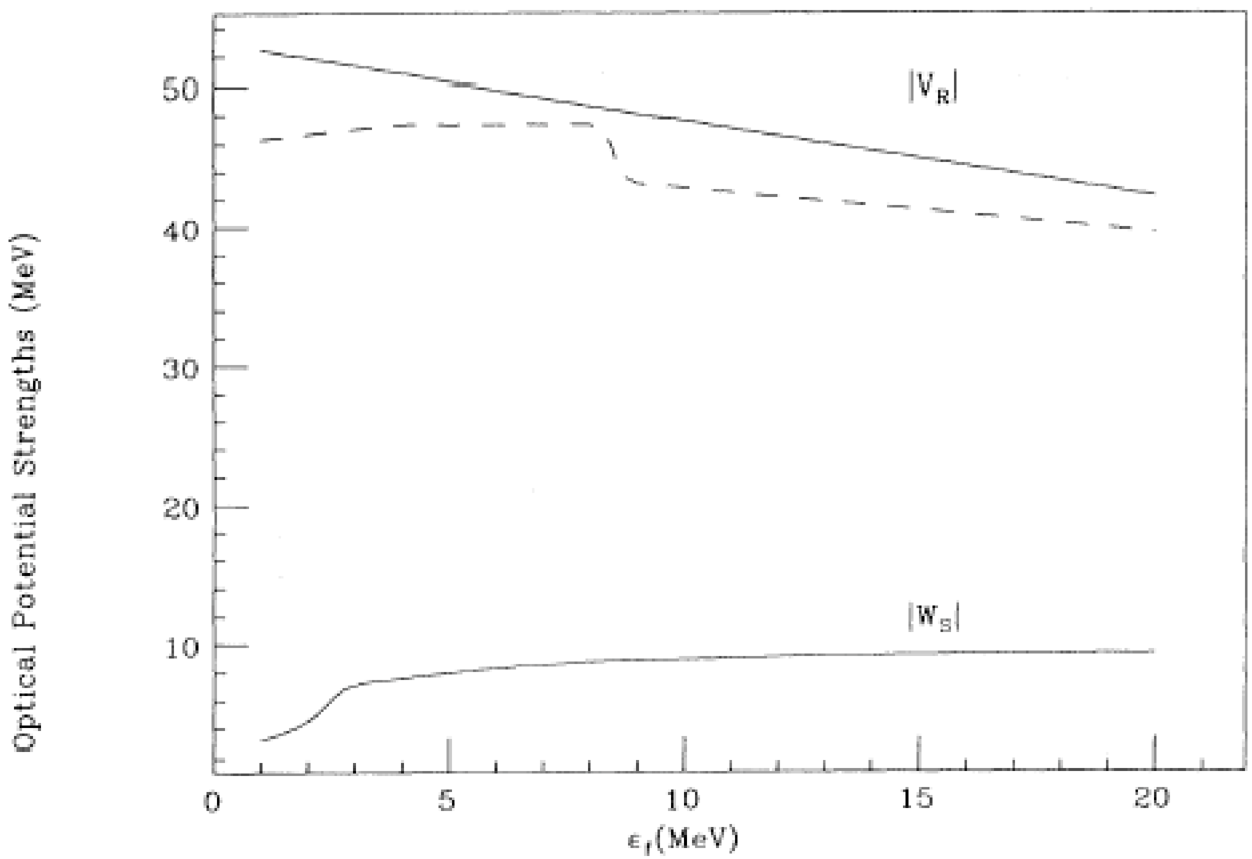

FIG. 2. Energy parametrization of the optical potential strengths for ^{120}Sn (solid curves) and ^{64}Ni (dashed curve).

$$\Gamma \approx \Gamma_0 + \Gamma^{\downarrow} ,$$

where

$$\Gamma_0 = \hbar P / T \qquad\qquad \Gamma^{\downarrow} = -2 \int \rho(r) W(r) \, d^3 r ,$$

TABLE I. Escape and spreading widths from Eqs. (3.2) and (3.5) in ^{208}Pb.

l_f	ε_{res} (MeV)	P	T (10^{-22} sec)	Γ_0 (MeV)	$\Gamma^{\downarrow}$ (M
7	3	0.10×10^{-3}	1.67	0.44×10^{-3}	3.36
7	5	0.38×10^{-2}	1.74	0.15×10^{-1}	4.15
7	7	0.35×10^{-1}	1.91	0.12	5.04
7	9	0.15	1.96	0.50	5.49
8	4	0.30×10^{-4}	1.46	0.13×10^{-3}	3.88
8	6	0.78×10^{-3}	1.54	0.30×10^{-2}	4.75
8	8	0.71×10^{-2}	1.63	0.28×10^{-1}	5.42
8	10	0.36×10^{-1}	1.68	0.14	6.09
9	14	0.05	1.51	0.20	6.99
9	16	0.13	1.69	0.49	7.29
9	18	0.27	1.79	0.97	7.51
9	20	0.45	2.20	1.34	7.36
10	18	0.04	1.34	0.19	8.53
10	20	0.09	1.41	0.45	8.39
10	22	0.20	1.55	0.86	8.75
10	24	0.35	1.72	1.35	8.69

TABLE IV. Initial-state parameters.

Initial state	ε_i (MeV)	γ_i (fm^{-1})	C^2S	C_i ($\mathrm{fm}^{-1/2}$)	l_i
$({}^{19}\mathrm{Ne}+n)_{2s_{1/2}}$	−16.86	0.901	0.56	20.99	0
$({}^{19}\mathrm{Ne}+n)_{1d_{5/2}}$	−17.10	0.907	1.03	7.75	2
$({}^{19}\mathrm{Ne}+n)_{1p_{1/2}}$	−17.14	0.908	1.96	10.42	1
$({}^{35}\mathrm{Ar}+n)_{1d_{3/2}}$	−15.25	0.857	2.92	11.12	2
$({}^{35}\mathrm{Ar}+n)_{2s_{1/2}}$	−16.43	0.877	2.5	30.87	0
$({}^{35}\mathrm{Ar}+n)_{2p_{3/2}}$	−17.88	0.915	0.12	36.94	1
$({}^{39}\mathrm{Ar}+n)_{1f_{7/2}}$	−9.87	0.681	0.54	2.69	3
$({}^{39}\mathrm{Ar}+n)_{2p_{3/2}}$	−11.14	0.732	0.1	16.67	1
$({}^{39}\mathrm{Ar}+n)_{1d_{3/2}}$	−11.39	0.741	2.2	7.17	2
$({}^{39}\mathrm{Ar}+n)_{2s_{1/2}}$	−12.25	0.768	1.26	21.07	0

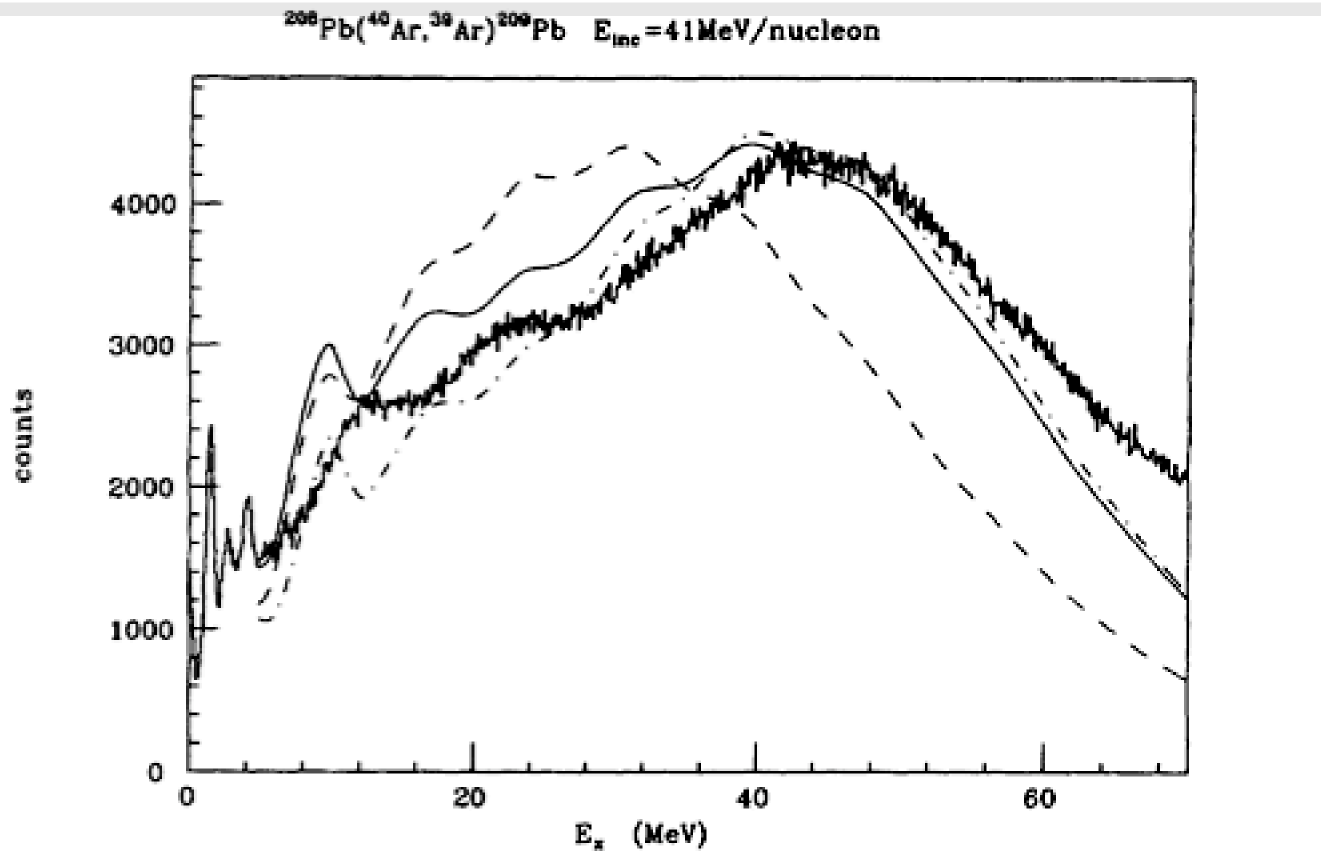

FIG. 7. Experimental spectrum of the reaction ^{208}Pb(^{40}Ar,^{39}Ar)^{209}Pb at $E_{\rm inc}$=41 MeV/nucleon compared to calculated spectra. The dashed line is the result of the calculation in which the spectra for all initial states shown in Fig. 6 have been summed. The solid line is the calculation in which the s state has been neglected, while the dot-dashed curve is the calculation including only the d state. All calculated spectra have been arbitrarily normalized to the data.

J of initial orbital determined by core momentum distributions.

A. B. and D.M. Brink, PRC44, 1559 (1991); PRC58, 2864 (1998), A.B,PRC60,546046

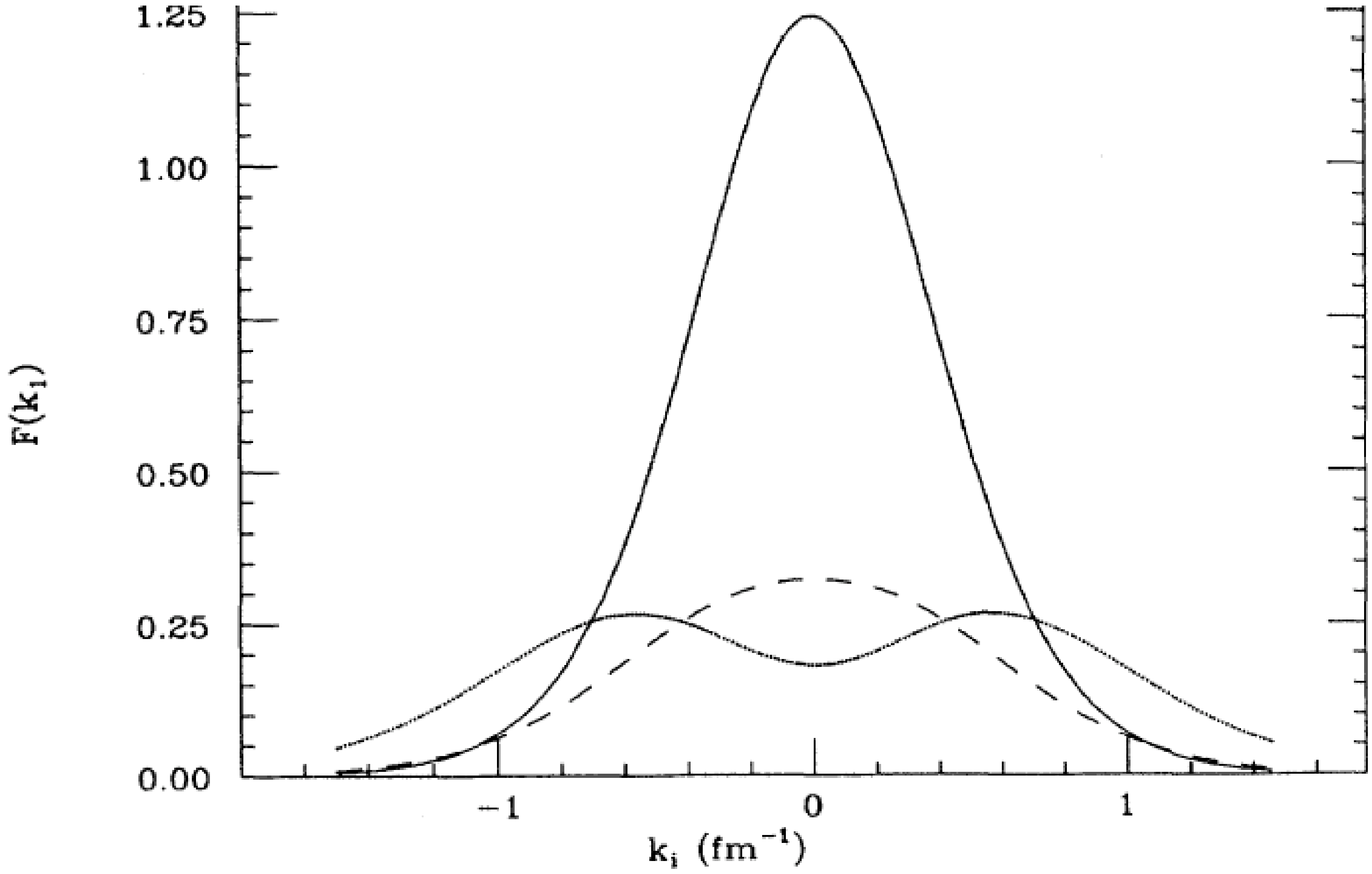

FIG. 11. Initial-state momentum distributions in ^{20}Ne according to Eq. (2.3a). The solid curve is for the $2s_{1/2}$ state, the dashed curve is the for $1p_{1/2}$, while the dotted curve is for the $1d_{5/2}$ state.

Istituto Nazionale di Fisica Nucleare
SEZIONE DI PISA

PHYSICAL REVIEW C, VOLUME 60, 054604

Initial state dependence of the breakup of weakly bound carbon isotopes

Angela Bonaccorso*

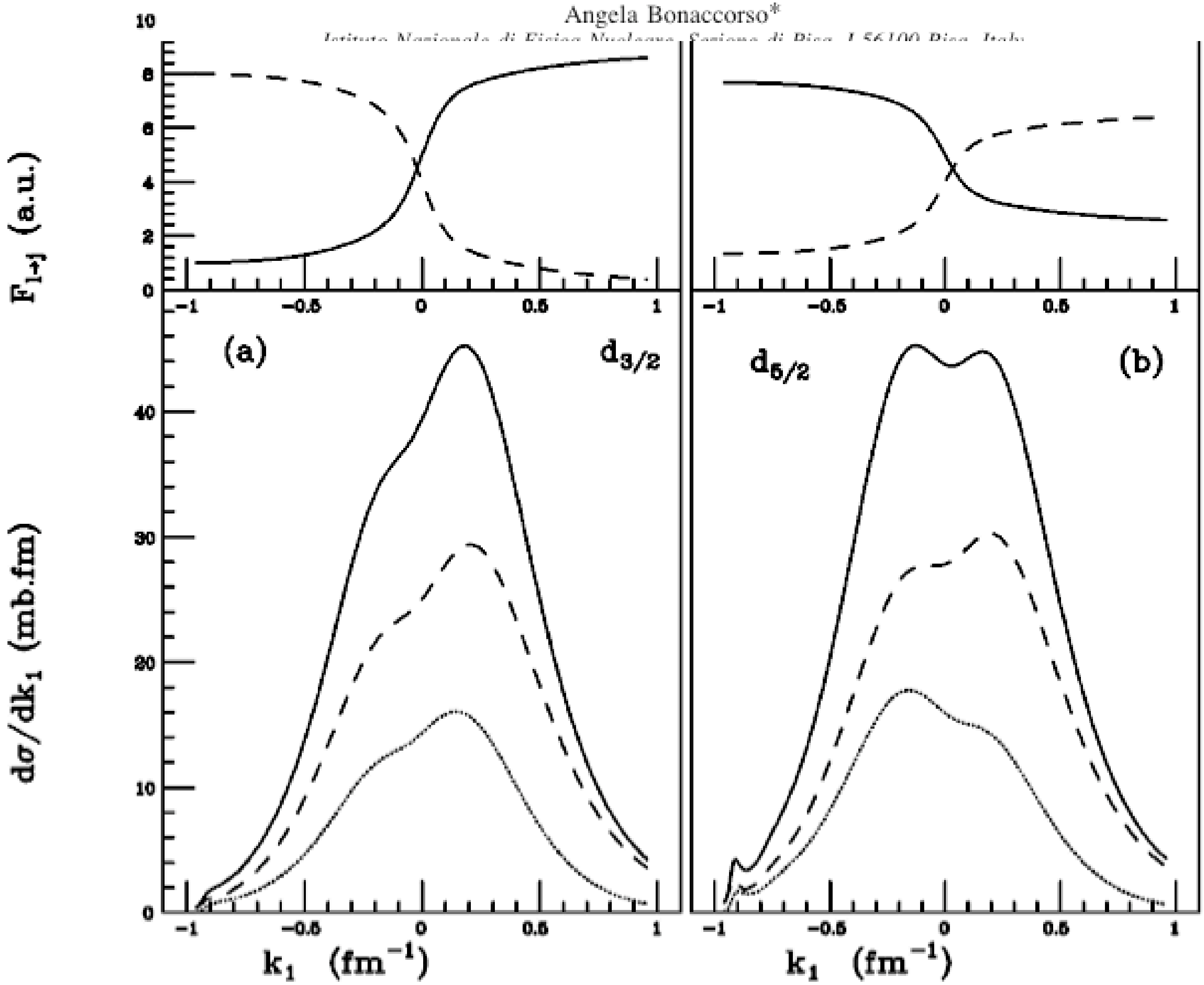

$^{19}C+^{9}Be$

88A.MeV

FIG. 3. The neutron final parallel distribution in the projectile reference frame for a d state at $E_{inc}=88A$ MeV. (a) $d_{3/2}$, $j_i=l_i-1/2$; (b) $d_{5/2}$, $j_i=l_i+1/2$. Top figures give the corresponding spin coupling coefficients $F_{l\to j}$ for $l_f=4$. Solid line $j_i\to j_f=l_f+1/2$, dashed line $j_i\to j_f=l_f-1/2$.

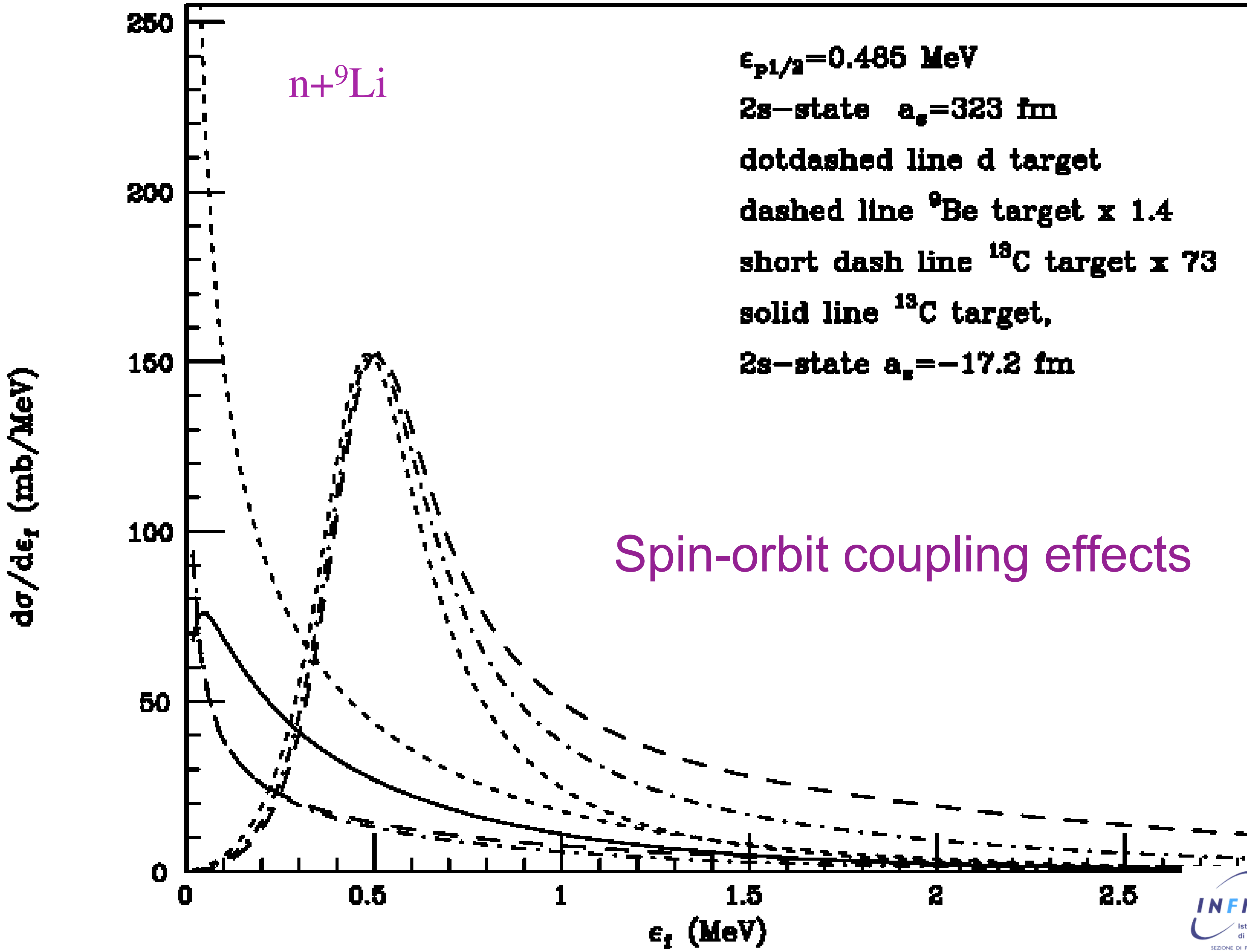

n+^{9}Li
$\epsilon_{p1/2}$=0.485 MeV
2s−state a_s=323 fm
dotdashed line d target
dashed line ^{9}Be target x 1.4
short dash line ^{13}C target x 73
solid line ^{13}C target,
2s−state a_s=−17.2 fm
Spin-orbit coupling effects
$d\sigma/d\epsilon_f$ (mb/MeV)
ϵ_f (MeV)
0
50
100
150
200
250
0.5
1
1.5
2
2.5